Prompt fission neutron spectra of ^{238}U and ^{232}Th above emissive fission threshold

V. M. Maslov,[1] Yu. V. Porodzinskij,[1] M. Baba,[2] A. Hasegawa,[3] N. V. Kornilov,[4] A. B. Kagalenko,[4] and N. A. Tetereva[1]
[1]*Joint Institute of Nuclear and Energy Research—"Sosny," 220109 Minsk, Belarus*
[2]*Cyclotron and Radioisotope Center, Tohoku University, Aramaki, Aza-Aoba, Aoba-ku, Sendai, Japan*
[3]*Japan Atomic Energy Research Institute, Tokai, Japan*
[4]*SSC RF Institute of Physics and Power Engineering, Obninsk, Russia*
(Received 13 March 2003; published 17 March 2004)

Statistical model calculations were performed to interpret the prompt fission neutron spectra (PFNS) from ^{238}U(n,f) and ^{232}Th(n,f) reactions for the incident neutron energies $E_n \sim 6-18$ MeV. Spectra of the prefission (presaddle) (n,xnf) reaction neutrons were calculated with Hauser-Feshbach statistical model, fission and (n,xn) reaction cross section data being described consistently. Spectra of neutrons, evaporated from the fission fragments, were approximated as a sum of two Watt distributions. The reduced neutron velocity in the center-of-mass system due to the neutron emission during fragment acceleration was assumed. PFNS component due to presaddle neutrons is evidenced in the shape of the measured PFNS data. We show it to be strongly correlated with the emissive fission contributions to the observed fission cross sections. The dependence of these contributions on the target nuclide fissility and incident neutron energy is shown to be pronounced in the PFNS shapes for ^{232}Th(n,f) and ^{238}U(n,f) reactions. High-energy tails of the first neutrons of (n,nf) and $(n,2nf)$ reactions are shown to be evidenced in the PFNS measured data trends.

DOI: 10.1103/PhysRevC.69.034607 PACS number(s): 24.75.+i, 25.85.Ec

I. INTRODUCTION

In neutron-induced fission of actinide nuclei one can distinguish between several neutron-emitting sources, along the path of the composite nucleus to the scission point. First, preequilibrium neutrons could be emitted before a composite system attains thermal equilibrium. Then presaddle neutrons might be evaporated before a composite system attains saddle-point deformation. This happens when incident neutron energy E_n is higher than the threshold E_{nnf} of (n,nf) emissive fission reaction ($E_{nnf} \sim 5-6$ MeV). Reaching saddle deformation, the nucleus rapidly transits from the saddle point to the "scission" point. Though this saddle-to-scission transition time is rather short ($\sim 10^{-21}$s) [1] "prescission" neutrons still could be emitted [2]. Notwithstanding the type of the neutrons emitted before fissioning nucleus reaches the scission point, either they are presaddle or prescission, the fission reaction looks like multiple-chance fission. This feature complicates a lot the analysis of the measured prompt fission neutron spectra, since the mass and excitation energy of the final fissioning nucleus are not known unambiguously. For neutron-induced fission of actinides at E_n up to ~ 20 MeV, (n,nf), $(n,2nf)$, and $(n,3nf)$ fission reactions contribute to the fission observables.

After scission, primary fission fragments may emit neutrons as well. Most of the neutrons are emitted from the fragments after full acceleration in their mutual Coulomb field. It was shown by Budtz-Jorgensen and Knitter [3] that this happens within $\sim 10^{-18}-10^{-17}$s. It might be assumed that some neutrons could be emitted just after scission [4], i.e., before full acceleration of the fission fragments. The angular distribution of these neutrons could be different from that of neutrons emitted from fully accelerated fragments, since their kinematical focusing is more similar to that of presaddle neutrons [4] emitted from the fissioning nucleus. Emission of neutrons during acceleration (preacceleration neutrons) might be possible if the neutron lifetime in excited fission fragments is comparable with the acceleration time of the fragments. Preacceleration neutron emission can be treated in the same way as an emission of the neutrons from the fission fragments after full acceleration. The angular distribution of the preacceleration neutrons will be focused along the fragments' direction of flight. However, the ratio of the yields of neutrons, emitted at 90° and at 0° relative to the fragments' direction of flight, will increase due to the reduced center-of-mass system (c.m.s.) velocity. The average energy of the prompt fission neutron spectrum $\langle E \rangle$ in the laboratory system (LS) could be estimated as $\langle E \rangle = \langle \varepsilon \rangle + E_v$, where $\langle \varepsilon \rangle$ is the average neutron energy in the c.m.s. and E_v is the c.m.s. energy per nucleon. Obviously, the latter value would be reduced because of the smaller kinetic energy of the fission fragments at the moment of preacceleration neutron emission.

Recent experimental investigations of the actinide [^{232}Th(n,f), ^{235}U(n,f), ^{238}U(n,f), and ^{237}Np(n,f)] prompt fission neutron spectra (PFNS) by Boykov *et al.* [5,6], Smirenkin *et al.* [7], and Lovchikova *et al.* [8] at $E_n \sim 13$, ~ 15, and ~ 18 MeV enhanced sufficiently the measured data base. It was observed in recent modeling of these PFNS data [8] that for incident neutron energies $E_n \sim 13-18$ MeV there was some excess of soft neutrons. It could be evidenced also as a lowering of the average energy values of PFNS $\langle \varepsilon \rangle$ (see also Ref. [9]) as compared with the estimates based on previous experimental data [10–13]. These peculiarities invoked speculations that modeling of the prompt fission neutron spectra in multiple-chance fission reactions, presaddle (n,xnf) neutron emission included, cannot reproduce the soft energy part of PFNS. These recent experimental investigations triggered also the assumptions that some prompt fission neutrons, other than presaddle neutrons or neutrons emitted from fission fragments, could be emitted from an additional neutron source (see Ref. [14]), However,

Svirin *et al.* [14] estimated prefission ^{238}U(n,xnf) reaction neutron spectra in a Weisscopf-Ewing approach, using a number of approximations regarding multiple-chance fission contributions and relevant parameters. In a recent analysis of emissive neutron spectra of ^{238}U$+n$ interaction by Kawano *et al.* [15], the authors successfully concentrated on the analysis of forward-peaked angular distribution of first neutrons for $E_n \lesssim 14$ MeV, fission neutron energy spectra being calculated with the model of Madland and Nix [16]. Kawano *et al.* [15] included preequilibrium emission of the first neutron in a proven quantum-mechanical approach. However, they used a rather approximate procedure to estimate multiple-chance fission contributions to the prompt fission neutron spectrum. Partitioning of the observed (n,F) fission cross section into (n,f), (n,nf), $(n,2nf)$, and $(n,3nf)$ nonemissive and emissive multiple-chance chance fission contributions, which was proposed in Ref. [15], could not give a consistent description of ^{238}U(n,f), ^{238}U$(n,2n)$, and ^{238}U$(n,3n)$ reaction data (see Ref. [9] for more details). Then, deriving prompt fission neutron spectrum from the analysis of inclusive neutron emission spectra, they assumed negligible contribution from the neutron spectra of $(n,2n)$ and $(n,3n)$ reactions at $E_n \sim 14$ MeV. That seems to be a rather strong assumption, which might be even less valid in case of a lower fissility target nuclide like ^{232}Th or higher incident neutron energies. Contributions of first, second, and third neutrons of $(n,2n)$ and $(n,3n)$ reactions to the neutron emission spectrum depend on the fission probabilities of the relevant nuclei, fissioning in multiple-chance fission reactions. We will illustrate this influence using ^{232}Th(n,f) and ^{238}U(n,f) reactions as examples.

We will estimate the contribution of presaddle (n,xnf) neutrons to the measured PFNS based on the description of ^{238}U(n,f), ^{238}U$(n,2n)$, ^{238}U$(n,3n)$, ^{232}Th(n,f), and ^{232}Th$(n,2n)$ reaction cross sections [17,18] with Hauser-Feshbach statistical model. We will analyze measured PFNS data for the ^{238}U(n,f) and ^{232}Th(n,f) reactions above and below emissive fission threshold and interpret major data trends. We suppose that following this approach the upper level of possible excess of soft neutrons could be more reliably estimated and then attributed to the influence of various factors, that may influence the postfission neutron spectra.

In our previous paper [9] we investigated several options to describe the PFNS data for ^{238}U(n,f) reaction in a multiple-chance fission excitation energy range, namely: (1) introduction of a prescission neutron source, (2) increase of (n,nf) and $(n,2nf)$ emissive fission chances contributions and relevant decrease of that of nonemissive first-chance fission, and (3) neutron emission from fission fragments before full acceleration.

The incorporation of the prescission neutron source could be of help, but its properties look rather contradictory, since its average neutron energy $[\langle\varepsilon\rangle \sim 0.5-0.6$ MeV$]$ is inconsistent with the time when total kinetic energy of fission fragments reaches $\sim$90% of its maximum value [3].

Prefission (or presaddle) neutrons emitted in (n,xnf) reactions strongly influence the shape of PFNS. We use calculated (n,xnf) reaction neutron spectra for the target nuclide A, which are strictly correlated with consistent (n,f) and (n,xn) cross sections' description [18]. Actually, the energy dependence of PFNS of $A+1$ composite nuclide for prompt fission neutron energies $\varepsilon \lesssim E_{th} \sim E_n - B_f$ resembles the shape of the fission probability P_f of A residual nuclide, B_f being the effective fission barrier value. The energy dependences of PFNS for most extensively studied target nuclides, i.e., ^{238}U and ^{232}Th for $\varepsilon \lesssim E_{th}$ resemble the shape of P_f of ^{238}U or ^{232}Th nuclides, respectively. Fission probabilities of residual nuclides ^{232}Th and ^{238}U are rather poorly investigated experimentally; they were defined by fitting relevant measured fission cross sections ^{232}Th(n,f) and ^{238}U(n,f) above (n,nf) emissive fission reaction thresholds. This was done simultaneously with (n,xn) reaction cross section description within Hauser-Feshbah approach. Any further increase of the contributions of ^{238}U(n,nf) [^{232}Th(n,nf)] or ^{238}U$(n,2nf)$ [^{232}Th$(n,2nf)$], which would add more soft neutrons to the calculated PFNS spectra, would either deteriorate the (n,xn) reaction cross section description or overshoot the experimental fission probability estimates of these A and $A-1$ residual nuclides.

Our assumption of neutron emission from fission fragments before full acceleration allows to describe measured PFNS data in the emitted neutron energy range of $\varepsilon \gtrsim 0.5$ MeV. However, the absolute value of the total kinetic energy at the moment of prompt fission neutron emission from the fragments seems to be larger than the values predicted based on the excitation energy of the fragments and acceleration time. Hence, the present approach might be considered as a phenomenological model viable to describe the observed energy dependence of PFNS for actinide nuclei.

II. PREFISSION (n,xnf) SPECTRA

We will analyze the measured PFNS data for ^{238}U(n,f) and ^{232}Th(n,f) reactions [5–8,12,13] above emissive fission threshold. Measured PFNS data for the ^{238}U(n,f) reaction at $E_n \sim 6$, 7, 8, 9, 13.2, 14.3, 14.7, 16, and 17.7 MeV and for the ^{232}Th(n,f) reaction at $E_n \sim 14.7$ and 17.7 MeV provide the possibility of observing that the variation of (n,nf) prefission neutron contribution depends on the excitation energy of the composite nucleus, as well as the target nuclide fissility. At E_n values below $(n,2nf)$ reaction threshold E_{n2nf} the contribution of (n,nf) reaction neutrons might be evidenced, while at highest incident neutron energy $E_n \sim 17.7$ MeV the first neutron of $(n,2nf)$ reaction also might be pronounced.

A. Multiple-chance fission

Contributions of (n,xnf) fission reactions to the observed (n,F) reaction cross section, coming from the fission of relevant equilibrated nuclei, are calculated in a Hauser-Feshbach approach, implemented in STAPRE statistical model code [19] as

$$\sigma_{nF}(E_n) = \sigma_{nf}(E_n) + \sum_{x=1}^{X} \sigma_{n,xnf}(E_n), \tag{1}$$

using fission probabilities $P_{fi}^{J\pi}(U)$ of relevant nuclei

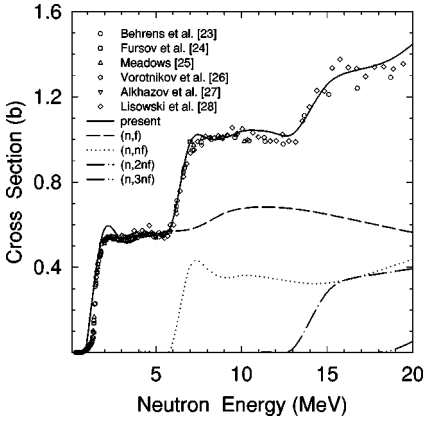

FIG. 1. $^{238}\mathrm{U}(n,F)$ fission cross section.

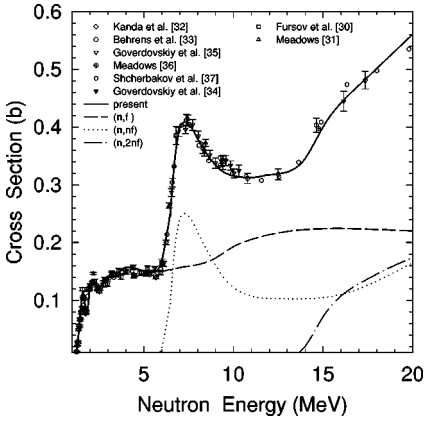

FIG. 2. $^{238}\mathrm{Th}(n,F)$ fission cross section.

$$\sigma_{n,xnf}(E_n) = \sum_{J\pi} \int_0^{U_{x+1}^{maax}} W_{x+1}^{J\pi}(U) P_{f(x+1)}^{J\pi}(U) dU. \qquad (2)$$

Here, $W_{x+1}^{J\pi}(U)$ is the population of $(x+1)$th residual nucleus at an excitation energy U after the emission of x neutrons; excitation energy U_{x+1}^{max} is defined by the incident neutron energy E_n and the energy removed from the composite system by (n,xnf) reaction neutrons. Fission probability $P_{fx}^{J\pi}$ of fissioning xth nucleus could be approximated as

$$P_{fx}^{J\pi}(E_n) = \frac{T_{fx}^{J\pi}(U)}{T_{fx}^{J\pi}(U) + T_{nx}^{J\pi}(U) + T_{\gamma x}^{J\pi}(U)}, \qquad (3)$$

where fission probability $P_{fx}^{J\pi}(E_n)$ depends on the $T_{fx}^{J\pi}$, $T_{nx}^{J\pi}(U)$, and $T_{\gamma x}^{J\pi}(U)$ transmission coefficients of fission, neutron emission, and radiative decay channels, respectively. Below we will omit nuclide index x in the equations.

In a double humped fission barrier model [20], neutron-induced fission process can be viewed as a two-step process, i.e., a successive crossing over the inner hump A and over the outer hump B. Hence, the transmission coefficient of the fission channel $T_f^{J\pi}(U)$ can be approximated [21,22] as

$$T_f^{J\pi}(U) = \frac{T_{fA}^{J\pi}(U) T_{fB}^{J\pi}(U)}{T_{fA}^{J\pi}(U) + T_{fB}^{J\pi}(U)}. \qquad (4)$$

Fission transmission coefficients $T_{fj}^{J\pi}(U)$ are defined by the level density $\rho_{fj}(\varepsilon, J, \pi)$ of the fissioning nucleus at the inner and outer saddles $(j=A,B)$,

$$T_{fj}^{J\pi}(U) = \int_0^U \frac{\rho_{fj}(\epsilon, J, \pi) d\epsilon}{\{1 + \exp[2\pi(E_{fj} + \epsilon - U)/\hbar\omega_j]\}}. \qquad (5)$$

Inner (outer) fission barrier height $E_{fA(B)}$ and width $\hbar\omega_{A(B)}$ are correlated with the saddle point asymmetries, which influence level density $\rho_{fA(B)}(\varepsilon, J, \pi)$ at saddle deformations, while the latter should influence the energy dependence of fission cross section.

Fission cross section data of $^{238}\mathrm{U}(n,F)$ and $^{232}\mathrm{Th}(n,F)$ reactions are compared with the calculated curves in Figs. 1 and 2. The contributions of xth multiple-chance fission reactions to the observed fission cross section $\beta_x(E_n) = \sigma_{n,xnf}(E_n)/\sigma_{nF}(E_n)$ and prefission neutron spectra $d\sigma_{n,xnf}^i/d\varepsilon, i=1,\ldots,x$ were calculated as well. Observed fission cross section data [23–28] for $^{238}\mathrm{U}(n,F)$ reaction (see Fig. 1) were described simultaneously with $^{238}\mathrm{U}(n,2n)$ and $^{238}\mathrm{U}(n,3n)$ reaction cross sections [18,29]. In case of $^{232}\mathrm{Th}+n$ interaction, $^{232}\mathrm{Th}(n,F)$ [30–37] (see Fig. 2) and $^{232}\mathrm{Th}(n,2n)$ reaction cross sections were described [38,39]. The preequilibrium first neutron emission [40,41] is important to reproduce consistently the observed (n,F) and (n,xn) reaction cross sections. Contributions of the $^{238}\mathrm{U}(n,f)$ (first-chance) fission reaction, $^{238}\mathrm{U}(n,nf)$ (second-chance) fission reaction, and $^{238}\mathrm{U}(n,2nf)$ (third-chance) fission reactions to the observed $^{238}\mathrm{U}(n,F)$ fission cross section are shown in Fig. 1. Figure 2 shows respective partial multiple-chance fission contributions to the observed $^{232}\mathrm{Th}(n,F)$ cross section. For incident neutron energies above emissive fission threshold first-chance nonemissive fission cross sections of $^{238}\mathrm{U}(n,f)$ and $^{232}\mathrm{Th}(n,f)$ reactions are rather weak functions of incident neutron energy. Second-chance $^{238}\mathrm{U}(n,nf)$ and third-chance $^{238}\mathrm{U}(n,2nf)$ fission reaction contributions are consistent with $^{237}\mathrm{U}(n,f)$ and $^{236}\mathrm{U}(n,f)$ fission cross sections in the first "plateau" regions, respectively.

Prefission (n,xnf) neutron emission lowers the excitation energy of residual $A,\ldots,A-x$ nuclei. Reducing the contribution of nonemissive first-chance fission and increasing the contribution of multiple-chance fission, we could reduce the average energy of $^{238}\mathrm{U}(n,F)$ PFNS down to the level predicted by Boykov *et al.* [5], Smirenkin *et al.* [7], and Lovchikova *et al.* [8]. Redistribution of multiple-chance fission contributions to the observed PFNS may mitigate the discrepancy of calculated PFNS with measured data (for details see Ref. [9]). There is only one option to reduce simultaneously nonemissive first-chance fission cross section [18] and increase (n,nf) and $(n,2nf)$ emissive fission contributions, leaving $(n,2n)$ and $(n,3n)$ reaction cross sections description unaffected. Since the behavior of the first-chance fission cross section σ_{f1} is obviously related to the energy dependence of the first-chance fission probability P_{f1}:

$$\sigma_{f1} = \sigma_r(1 - q(E_n))P_{f1}, \qquad (6)$$

its contribution to the observed fission cross section could be lowered by decreasing the first-chance fission probability

P_{f1}. The increase of the contribution of the first neutron preequilibrium emission $q(E_n)$ will deteriorate $(n,2n)$ and $(n,3n)$ cross sections' description drastically. First-chance fission probability P_{f1} depends on the level density parameters of fissioning $A+1$ residual A nuclides. First-chance fission probability P_{f1} could be decreased assuming negative shell correction value at the outer saddle, i.e., $\delta W_f \sim -1.6$ MeV, as compared with $\delta W_f \sim 0.6$ MeV [21]. Total fission cross section could be kept unaffected, since decreased contribution of the first-chance fission cross section σ_{f1} could be compensated by increasing fission probabilities of A and $(A-1)$ nuclides. In that case cross sections of $(n,2n)$ and $(n,3n)$ reactions also would be reproduced. We have shown recently [9] that for $E_n = 16$ MeV increased contribution of the multiple-chance fission reactions leads to the increase of the contribution of soft neutrons. However, at higher prompt fission neutron energies $\varepsilon \gtrsim 4$ MeV calculated PFNS shape still remains incompatible with measured data trend. Note that contribution of second-chance fission reaction $^{238}\mathrm{U}(n,nf)$ keeps increasing at $E_n \gtrsim 14$ MeV, while Kawano *et al.* [15] predict its sharp lowering with subsequent strong increase of $^{238}\mathrm{U}(n,2nf)$ third-chance fission contribution. Decreasing trend of nonemissive fission cross section of $^{238}\mathrm{U}(n,f)$, as well as high contributions of second-chance $^{238}\mathrm{U}(n,nf)$ and third-chance $^{238}\mathrm{U}(n,2nf)$ to the observed fission cross section of $^{238}\mathrm{U}$, predicted by Kawano *et al.* [15], deteriorate the consistent description of $^{238}\mathrm{U}(n,f)$ and $^{238}\mathrm{U}(n,xn)$ reaction cross sections. In other words, we argue that estimates of multiple-chance fission contributions, different from that shown in Fig. 1, would either deteriorate the consistent description of $^{238}\mathrm{U}(n,F)$, $^{238}\mathrm{U}(n,2n)$, and $^{238}\mathrm{U}(n,3n)$ or nonemissive $^{237}\mathrm{U}(n,f)$ and $^{236}\mathrm{U}(n,f)$ reaction cross sections. The same conclusion applies in the case of ^{232}Th target nuclide.

B. First neutron spectrum

First neutron spectrum of (n,nx) reaction is calculated in a statistical Hauser-Feshbach theory of nuclear reactions as

$$\frac{d\sigma^1_{nnx}}{d\varepsilon} = \sum_{J\pi} W^A(E_n-\varepsilon, J^\pi). \tag{7}$$

Here, $W^A(E_n-\varepsilon, J^\pi)$ is the population of the excited states in residual nuclide A, formed after emission of the first neutron with energy ε, spin J, and parity π at excitation energy $E_n - \varepsilon$. For the compound nucleus $A+1$ the excitation energy equals $U=E_n+B_n^{A+1}$, where B_n^{A+1} is the neutron binding energy in a composite nuclide $A+1$. First neutron spectrum contains the contribution of the preequilibrium neutron emission, for details of preequilibrium model calculations see Ref. [18]. Present statistical model of fission reaction assumes fission/neutron evaporation competition during decay of the excited compound nucleus, which is formed after the first-chance emission of preequilibrium neutron [19], treated with a simple version of exciton model [40,41]. The equilibration is treated with a set of master equations, describing the evolution of the excited nucleus states, classified by the number of particles plus holes [19].

To simplify the equations, we will omit spin and parity indices for fission Γ_f, neutron Γ_n, γ emission Γ_γ, and total $\Gamma=\Gamma_n+\Gamma_\gamma+\Gamma_f$ widths, as well as summations over J and π, made according to the spin and parity conservation laws in neutron emission cascades. Neutron spectrum $d\sigma^1_{nnf}/d\varepsilon$ of the $(n,nf)^1$ reaction could be calculated using the first neutrons spectrum of (n,nx) reaction, i.e., $(n,nx)^1$, multiplied by the fission probability of nuclide A,

$$\frac{d\sigma^1_{nnf}}{d\varepsilon} = \frac{d\sigma^1_{nnx}}{d\varepsilon}\frac{\Gamma_f^A(E_n-\varepsilon)}{\Gamma^A(E_n-\varepsilon)}. \tag{8}$$

The hard-energy tail of the neutron spectrum $d\sigma^1_{nnf}/d\varepsilon$ of the $(n,nf)^1$ reaction would resemble the fission probability shape of nuclide A.

Spectrum of the first neutrons $d\sigma^1_{n2nx}/d\varepsilon$ of $(n,2nx)$ reaction, which we denote $(n,2nx)^1$, could be obtained using the first neutrons spectrum of (n,nx) reaction, i.e., $(n,nx)^1$ [see Eq. (7)], multiplied by the neutron emission probability of nuclide A,

$$\frac{d\sigma^1_{n2nx}}{d\varepsilon} = \frac{d\sigma^1_{nnx}}{d\varepsilon}\frac{\Gamma_n^A(E_n-\varepsilon)}{\Gamma^A(E_n-\varepsilon)}. \tag{9}$$

Spectrum of the first neutrons $d\sigma^1_{n2nf}/d\varepsilon$ of $(n,2nf)^1$ reaction, i.e., $(n,2nf)^1$, is obtained integrating the first neutrons spectrum of $(n,2nx)$ reaction, i.e., $(n,2nx)^1$, multiplied by the fission probability of nuclide $(A-1)$,

$$\frac{d\sigma^1_{n2nf}}{d\varepsilon} = \int_0^{E_n-B_n^A} \frac{d\sigma^1_{n2nx}}{d\varepsilon}\frac{\Gamma_f^{A-1}(E_n-B_n^A-\varepsilon-\varepsilon_1)}{\Gamma^{A-1}(E_n-B_n^A-\varepsilon-\varepsilon_1)}d\varepsilon_1. \tag{10}$$

The hard-energy tail of the first neutron spectrum $d\sigma^1_{n2nf}/d\varepsilon$ of the $(n,2nf)$ reaction would resemble the fission probability shape of $(A-1)$ nuclide.

Spectrum of the first neutrons $d\sigma^1_{n3nx}/d\varepsilon$ of $(n,3nx)$ reaction, which we denote $(n,3nx)^1$, is obtained integrating the first neutrons spectrum of $(n,2nx)$ reaction, i.e., $(n,2nx)^1$ [see Eq. (9)], using the neutron emission probability of $(A-1)$ nuclide as

$$\frac{d\sigma^1_{n3nx}}{d\varepsilon} = \int_0^{E_n-B_n^A} \frac{d\sigma^1_{n2nx}}{d\varepsilon}\frac{\Gamma_n^{A-1}(E_n-B_n^A-\varepsilon-\varepsilon_1)}{\Gamma^{A-1}(E_n-B_n^A-\varepsilon-\varepsilon_1)}d\varepsilon_1. \tag{11}$$

Then, having the spectrum of the first neutron of the $(n,3nx)$ reaction, $d\sigma^1_{n3nf}/d\varepsilon$ spectrum of first neutrons of $(n,3nf)$ reaction, i.e., $(n,3nf)^1$, could be calculated as

$$\frac{d\sigma^1_{n3nf}}{d\varepsilon} = \int_0^{E_n-B_n^A-B_n^{A-1}} \frac{d\sigma^1_{n3nx}}{d\varepsilon} \times \frac{\Gamma_f^{A-2}(E_n-B_n^A-B_n^{A-1}-\varepsilon-\varepsilon_1-\varepsilon_2)}{\Gamma^{A-2}(E_n-B_n^A-B_n^{A-1}-\varepsilon-\varepsilon_1-\varepsilon_2)}d\varepsilon_2. \tag{12}$$

The latter equation is actually a double integral, which is obtained after substitution of Eq. (11) into Eq. (12), the integrations are maintained over the energies of partial neutrons of $(n,3nf)$ reaction.

C. Second neutron spectra

Second neutron spectrum of the $(n,2nx)$ reaction, $(n,2nx)^2$, i.e., emission spectrum of the second neutrons or neutrons, emitted from residual nuclide A, is calculated integrating over first neutron spectrum $(n,nx)^1$ of the (n,nx) reaction [see Eq. (7)] using the neutron emission probability of nuclide A as

$$\frac{d\sigma^2_{n2nx}}{d\varepsilon} = \int_0^{E_n - B_n^A} \frac{d\sigma^1_{nnx}}{d\varepsilon} \frac{\Gamma_n^A(E_n - B_n^A - \varepsilon_1)}{\Gamma^A(E_n - B_n^A - \varepsilon_1)} d\varepsilon_1. \quad (13)$$

Second neutron spectrum of the $(n,2nf)$ reaction, which we denote $(n,2nf)^2$, would be expressed as a double integral. It would be obtained using Eq. (13), which defines second neutron spectrum of $(n,2nx)$ reaction, i.e., $(n,2nx)^2$ and fission probability of $(A-1)$ nuclide as

$$\frac{d\sigma^2_{n2nf}}{d\varepsilon} = \int_0^{E_n - B_n^A} \frac{d\sigma^2_{n2nx}}{d\varepsilon} \frac{\Gamma_f^{A-1}(E_n - B_n^A - \varepsilon_1 - \varepsilon_2)}{\Gamma^{A-1}(E_n - B_n^A - \varepsilon_1 - \varepsilon_2)} d\varepsilon_2. \quad (14)$$

Obviously, boundary energies of first and second neutrons of $(n,2nf)$ reactions coincide.

Second neutron spectrum of the $(n,3nx)$ reaction, which we denote $(n,3nx)^2$, also would be a double integral, it is defined using second neutron spectrum of $(n,2nx)$ reaction, i.e., $(n,2nx)^2$ [see Eq. (13)] and neutron emission probability of $(A-1)$ nuclide as

$$\frac{d\sigma^2_{n3nx}}{d\varepsilon} = \int_0^{E_n - B_n^A} \frac{d\sigma^2_{n2nx}}{d\varepsilon} \frac{\Gamma_n^{A-1}(E_n - B_n^A - \varepsilon_1 - \varepsilon_2)}{\Gamma^{A-1}(E_n - B_n^A - \varepsilon_1 - \varepsilon_2)} d\varepsilon_2. \quad (15)$$

Second neutron spectrum of the $(n,3nf)$ reaction, which we denote $(n,3nf)^2$, is calculated integrating second neutron spectrum of $(n,3nx)$ reaction, $(n,3nx)^2$, which is a double integral, and a fission probability of $(A-2)$ nuclide

$$\frac{d\sigma^2_{n3nf}}{d\varepsilon} = \int_0^{E_n - B_n^A - B_n^{A-1}} \frac{d\sigma^2_{n3nx}}{d\varepsilon} \times \frac{\Gamma_f^{A-2}(E_n - B_n^A - B_n^{A-1} - \varepsilon_1 - \varepsilon_2 - \varepsilon_3)}{\Gamma^{A-2}(E_n - B_n^A - B_n^{A-1} - \varepsilon_1 - \varepsilon_2 - \varepsilon_3)} d\varepsilon_3. \quad (16)$$

The latter expression is a triple integral over excitation energies of the $(A-2)$, $(A-1)$, and A residual nuclides, or, equivalently, over partial neutron energies of $(n,3nf)$ reaction.

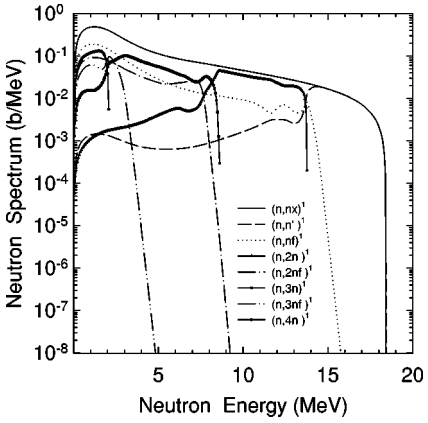

FIG. 3. Components of the first neutron spectrum of ^{238}U(n,F) reaction for incident neutron energy 20 MeV.

D. Third neutron spectra

Third neutrons spectrum of the $(n,3nx)$ reaction, $(n,3nx)^3$, is obtained from $(n,2nx)^2$ [see Eq. (13)] reaction spectrum using neutron emission probability from $(A-1)$ nuclide as

$$\frac{d\sigma^3_{n3nx}}{d\varepsilon} = \int_0^{E_n - B_n^A - B_n^{A-1}} \frac{d\sigma^2_{n2nx}}{d\varepsilon} \times \frac{\Gamma_n^{A-1}(E_n - B_n^A - B_n^{A-1} - \varepsilon_1 - \varepsilon_2)}{\Gamma^{A-1}(E_n - B_n^A - B_n^{A-1} - \varepsilon_1 - \varepsilon_2)} d\varepsilon_2. \quad (17)$$

The latter spectrum is a double integral over excitation energies of A and $(A-1)$ residual nuclides, or, equivalently, over partial neutron energies of $(n,3nx)$ reaction.

Third neutrons spectrum $(n,3nf)^3$ is obtained using the third neutrons spectrum of $(n,3nx)$ reaction, $(n,3nx)^3$, and fission probability of $(A-2)$ nuclide as

$$\frac{d\sigma^3_{n3nf}}{d\varepsilon} = \int_0^{E_n - B_n^A - B_n^{A-1}} \frac{d\sigma^3_{n3nx}}{d\varepsilon} \times \frac{\Gamma_f^{A-2}(E_n - B_n^A - B_n^{A-1} - \varepsilon_1 - \varepsilon_2 - \varepsilon_3)}{\Gamma^{A-2}(E_n - B_n^A - B_n^{A-1} - \varepsilon_1 - \varepsilon_2 - \varepsilon_3)} d\varepsilon_3. \quad (18)$$

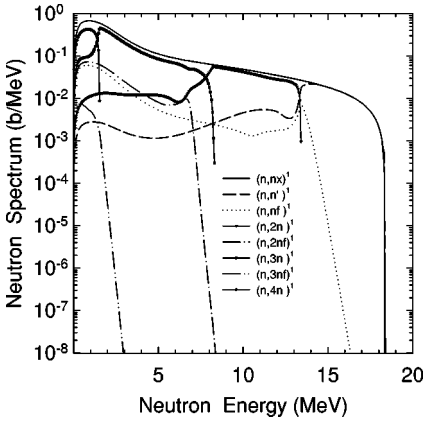

FIG. 4. Components of the first neutron spectrum of ^{232}Th(n,F) reaction for incident neutron energy 20 MeV.

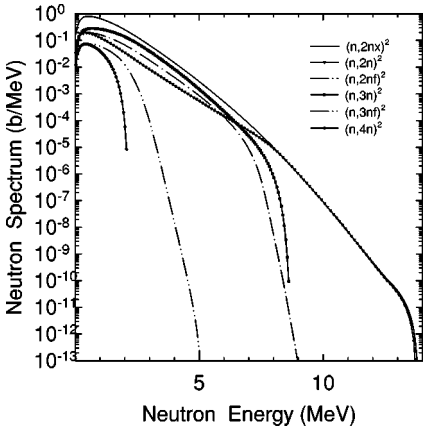

FIG. 5. Components of the second neutron spectrum of ^{238}U(n,F) reaction for incident neutron energy 20 MeV.

The latter expression is a triple integral over excitation energies of the $(A-2)$, $(A-1)$, and A residual nuclides, or, equivalently, over partial neutron energies of $(n,3nf)$ reaction.

E. Partial neutron spectra of U and Th nuclei

Partial (n,xnf) reaction neutron spectra for $E_n=20$ MeV are presented on Figs. 3–8. Figures 3 and 4 show the first neutron spectra for ^{238}U$+n$ and ^{232}Th$+n$ interactions. Obviously, neutron/fission competition is defined by the level density and fission barrier parameters of relevant fissioning and residual nuclei.

In case of ^{238}U$+n$ and ^{232}Th$+n$ interactions, first neutron spectra of $(n,n\gamma)$, $(n,2n\gamma)$, and $(n,3n\gamma)$ reactions have similar shapes; they demonstrate characteristic lowering of the soft neutron energy parts, which is due to the competition either of first or higher chance fission reactions with emission of second or third neutrons in relevant reactions. Relative contributions of first neutron spectra of $(n,n\gamma)$ reaction to the first neutron spectrum of (n,nx) reaction are correlated with γ-emission/neutron/fission competition for the residual nuclei, which are not much different for the ^{238}U$+n$ and ^{232}Th$+n$ interactions.

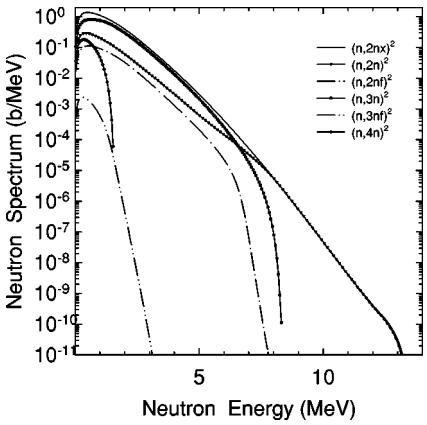

FIG. 6. Components of the second neutron spectrum of ^{232}Th(n,F) reaction for incident neutron energy 20 MeV.

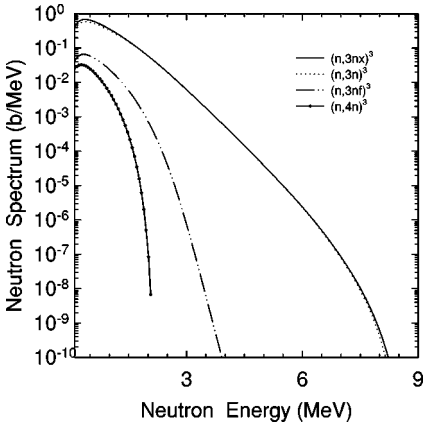

FIG. 7. Components of the third neutron spectrum of ^{238}U(n,F) reaction for incident neutron energy 20 MeV.

Shapes of the $(n,nf)^1$ spectra $d\sigma^1_{nnf}/d\varepsilon$ for ^{238}U(n,f) and ^{232}Th(n,f) reactions are defined by the fission probabilities of ^{238}U and ^{232}Th nuclides, respectively. Figures 1 and 2 demonstrate that contributions of (n,nf) second-chance fission reaction to the observed fission cross sections are rather different in case of ^{238}U and ^{232}Th target nuclides. Cross section shape of ^{238}U(n,nf) reaction is rather flat above the relevant threshold E_{nnf}, while that of ^{232}Th(n,nf) reaction demonstrates rather strong dependence on the incident neutron energy. Broad peak in ^{232}Th(n,nf) reaction cross section is pronounced in the neutron spectrum of (n,nf) reaction (see Fig. 4). Sharp decrease of ^{232}Th$(n,nf)^1$ reaction spectrum for emitted first neutron energies $\varepsilon \gtrsim E_n - B_f$ would be evidenced in measured prompt fission neutron spectrum (see below).

In case of ^{238}U$+n$ interaction, $(n,2nf)^1$ spectrum $d\sigma^1_{n2nf}/d\varepsilon$ contribution is lower than that of $(n,nf)^1$ reaction up to $\varepsilon \sim 5$ MeV; for $\varepsilon \gtrsim 5$ MeV it turns out to be higher (see Fig. 3). Contribution of $(n,2nf)^1$ reaction spectrum to the first neutron spectrum of ^{232}Th$+n$ interaction is systematically higher than that of $(n,nf)^1$ spectrum for $\varepsilon \lesssim 8$ MeV (see Fig. 4).

In case of ^{238}U, target nuclide contribution of $(n,3nf)^1$ reaction spectra $d\sigma^1_{n3nf}/d\varepsilon$ to the first neutron spectrum is

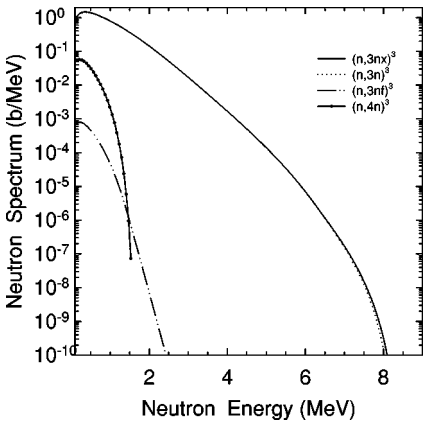

FIG. 8. Components of the third neutron spectrum of ^{232}Th(n,F) reaction for incident neutron energy 20 MeV.

comparable with those of lower chance fission reactions for $\varepsilon \lesssim 3$ MeV, while in case of ^{232}Th target nuclide it is much lower (see Figs. 3 and 4).

Second neutron spectrum of $(n,2nf)^2$ reaction contribution to the spectrum of second neutrons of $(n,2nx)^2$ reaction is relatively higher in case of ^{238}U$+n$ interaction, than in case of lower fissility target ^{232}Th (see Figs. 5 and 6). In case of ^{238}U$+n$ interaction the second neutron spectrum of $(n,2nf)^2$ reaction contribution to the spectrum of second neutron of $(n,2nx)^2$ reaction is higher than that of $(n,2n\gamma)^2$ (see Fig. 5), but lower than that of $(n,3n\gamma)^2$ reaction for $\varepsilon \lesssim 9$ MeV. In case of lower fissility target nuclide ^{232}Th, $(n,2nf)^2$ third-chance fission reaction contribution to the spectrum of second neutron of $(n,2nx)^2$ reaction is lower than both $(n,2n\gamma)^2$ and $(n,3n\gamma)^2$ contributions (see Fig. 6). Second neutron spectrum of $(n,3nf)^2$ reaction contribution to the $(n,2nx)^2$ reaction spectrum also seems to keep direct dependence on the target nuclide fissility. For the lower fissility target ^{232}Th nuclide it is much lower than in case of ^{238}U target nuclide (see Figs. 5 and 6).

Main contribution to the third neutron spectrum $(n,3nx)^3$ comes from $(n,3n\gamma)$ reaction (see Figs. 7 and 8) for both target nuclei. The contribution of $(n,3nf)^3$ is higher in case of ^{238}U target (see Fig. 7) than in case of ^{232}Th (see Fig. 8). Because of the lowering of excitation energy after emission of first and second neutrons, influence of the level density of relevant nuclei and fission barrier parameters for the third neutron spectra is much higher than in case of first or second neutron emission.

Summarizing, we anticipate that partial (n,xnf) prefission neutron spectra for different target nuclei would be pronounced in observed PFNS for the target nuclides with different fissilities to a different extent. Present estimates of the partial prefission neutron spectra, calculated simultaneously with consistent reproduction of (n,f) and (n,xn) reaction cross sections, are more reliable than various previous estimates, based on Weisscopf-Ewing approach [14,42], or more ambiguous phenomenological estimates of prefission neutron spectra, which are used in previous PFNS analyses [16,15].

III. MODEL FOR PFNS CALCULATION

A. PFNS for multiple-chance fission

At incident neutron energies above emissive fission threshold and up to $E_n=20$ MeV, prompt fission neutron spectra $S(\varepsilon,E_n)$ are calculated as a superposition of (n,xnf) prefission neutron spectra $d\sigma^k_{nxnf}/d\varepsilon(x=1,2,3,\text{or } 4;k=1,2,\ldots,x)$ and postfission spectra $S_{A+2-x}(\varepsilon,E_n)$ of neutrons, evaporated from fission fragments:

$$
\begin{aligned}
S(\varepsilon,E_n) &= \widetilde{S}_{A+1}(\varepsilon,E_n)+\widetilde{S}_{A}(\varepsilon,E_n)+\widetilde{S}_{A-1}(\varepsilon,E_n)+\widetilde{S}_{A-2}(\varepsilon,E_n)\\
&= \nu^{-1}(E_n)\Bigg\{\nu_1(E_n)\beta_1(E_n)S_{A+1}(\varepsilon,E_n)+\beta_2(E_n)\\
&\quad\times\left[\nu_2(E_n-\langle E_{nnf}\rangle)S_A(\varepsilon,E_n)+\frac{d\sigma^1_{nnf}}{d\varepsilon}\right]\\
&\quad+\beta_3(E_n)\left[\nu_3(E_n-B^A_n-\langle E^1_{n2nf}\rangle\right.\\
&\quad\left.-\langle E^2_{n2nf}\rangle)S_{A-1}(\varepsilon,E_n)+\left(\frac{d\sigma^1_{n2nf}}{d\varepsilon}+\frac{d\sigma^2_{n2nf}}{d\varepsilon}\right)\right]\\
&\quad+\beta_4(E_n)\left[\nu_4(E_n-B^A_n-B^{A-1}_n-\langle E^1_{n3nf}\rangle-\langle E^2_{n3nf}\rangle\right.\\
&\quad\left.-\langle E^3_{n3nf}\rangle)S_{A-2}(\varepsilon,E_n)\right.\\
&\quad\left.+\left(\frac{d\sigma^1_{n3nf}}{d\varepsilon}+\frac{d\sigma^2_{n3nf}}{d\varepsilon}+\frac{d\sigma^3_{n3nf}}{d\varepsilon}\right)\right]\Bigg\}. \qquad (19)
\end{aligned}
$$

$\widetilde{S}_{A+2-x}(\varepsilon,E_n)$ denote contributions to the observed prompt fission neutron spectra, which could be traced to multiple-chance fission reactions, $\langle E^k_{nxnf}\rangle$ is the kth neutron average energy $(k\leqslant x)$ of the (n,xnf)-reaction neutron spectrum $d\sigma^k_{nxnf}/d\varepsilon$.

Number of prompt fission neutrons $\nu(E_n)$ is estimated as

$$\nu(E_n)=\sum_{x=1}^{X}\{[\nu_x(E_{nx})+(x-1)]\beta_x(E_n)\}, \qquad (20)$$

subscript $x=1,\ldots,X$ denotes multiple-chance fission of $A+1$, A, $A-1$, and $A-2$ nuclides after emission of $(x-1)$ prefission neutrons; $\beta_x(E_n)$ is the contribution of xth chance fission to the observed fission cross section; $\nu_x(E_{nx})$ is the prompt fission neutron number for the xth chance fission reaction.

Spectra $S_{A+2-x}(\varepsilon,E_n)$ of neutrons, evaporated from fission fragments of $(A+2-x)$ fissioning nucleus were approximated as a superposition of two Watt distributions, taken with equal weights [43]:

$$S_x(\varepsilon,E_n)=0.5\sum_{j=1}^{2}W_i(\varepsilon,E_n,T_{ij}(E_n),\alpha), \qquad (21)$$

$$W_x(\varepsilon,E_n,T_{ij}(E_n),\alpha)=\frac{2}{\sqrt{\pi}T_{ij}^{3/2}}\sqrt{\varepsilon}\exp\left(-\frac{\varepsilon+\widetilde{E}_{vxj}}{T_{ij}}\right)\frac{sh(\sqrt{b_{xj}\varepsilon})}{\sqrt{b_{ij}\varepsilon}}, \qquad (22)$$

$$b_{xj}=\frac{4\widetilde{E}_{vij}}{T_{ij}^2},\quad T_{xj}=k_{xj}\sqrt{E^*_x}=k_{xj}\sqrt{E_r-TKE_x+U_x}. \qquad (23)$$

T_{xj} is the temperature parameter for light and heavy fragments $(j=l,h)$ of xth nucleus, α is the ratio of the total kinetic energy (TKE) at the moment of neutron emission to the appropriate TKE value at the full acceleration limit, E_r is the energy release in fission. In Watt's equation [Eq. (22)] c.m.s. energy per nucleon is reduced as $\widetilde{E}_{vxj}=\alpha E_{vxj}$, $\widetilde{E}_{vxl}=(A_{hx}/A_{lx}A_x)\alpha\times\text{TKE}_x$, $\widetilde{E}_{vxh}=(A_{lx}/A_{hxi}A_x)\alpha\times\text{TKE}_x$. The ratio of the "temperatures" for light and heavy fragments $r=1.248$ is the semiempirical fitting parameter, which was assumed to be independent of the target nucleus, k_{xj} is the parameter obviously related with the main level density parameter [43].

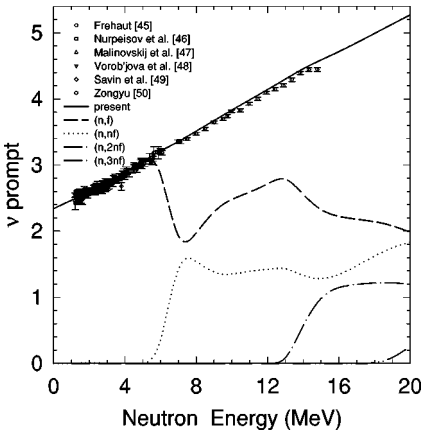

FIG. 9. Prompt fission neutron number of $^{238}\mathrm{U}(n,F)$ reaction.

We take into account prefission neutrons' influence on the fission fragments' excitation energy, reducing it by the average energies of prefission neutrons and relevant neutron binding energies B_x, i.e., U_x for the nucleus $A_x=A+2-x$ after emission of $(x-1)$ neutrons was calculated as

$$U_x = E_n + B_n - \sum_{j\leqslant x} (\langle E_{xj}\rangle + B_x). \tag{24}$$

The excitation energy of fission fragments of fissioning nucleus with mass number $A+2-x$ equals $E_x^*=E_r-\mathrm{TKE}+U_x$, fission fragment temperature parameters $T_{xj}(E_n)$ versus excitation energy are defined for each fissioning nucleus. Below emissive fission threshold, this approximation allows to get better agreement with measured data on actinide PFNS [43]. The systematic approach of Ref. [44] was used to estimate partial prompt neutron multiplicities ν_x below emissive fission threshold.

B. Neutron multiplicity

Neutron multiplicities $\nu_x(E_{nx})$ define relative contributions of the (n,xnf) prefission neutron spectra $d\sigma^k_{nxnf}/d\varepsilon$ ($x=1$, 2, 3, or 4; $k=1,2,\ldots,x$) and postfission spectra $S_{A+2-x}(\varepsilon,E_n)$ in $\widetilde{S}_{A+2-x}(\varepsilon,E_n)$ [see Eq. (19)]. We assumed that the excitation

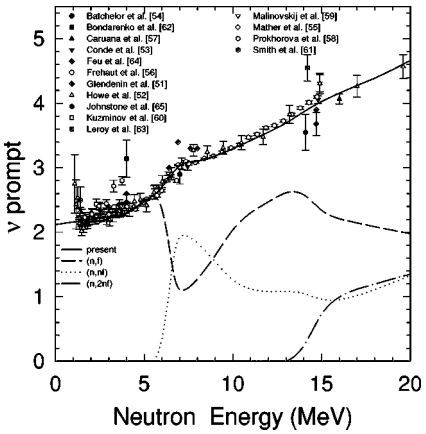

FIG. 10. Prompt fission neutron number of $^{232}\mathrm{Th}(n,F)$ reaction.

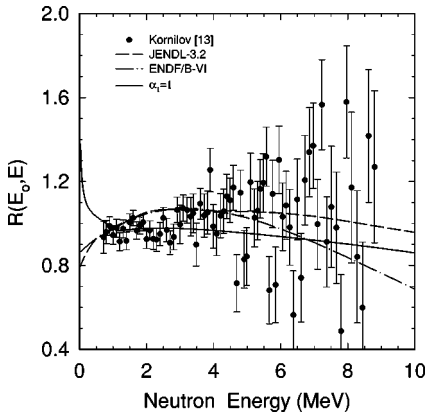

FIG. 11. Measured and calculated $^{238}\mathrm{U}(n,F)$ reaction PFNS at $E_n=6$ MeV relative to Maxwell PFNS with the average energy $\langle E\rangle=2.0367$ MeV.

energy U_x [Eq. (24)] is brought into nucleus A_x in the reaction $n+A_{x-1}\rightarrow$ fission. Incident neutron energy E_{nx} for the multiple-chance fission reactions is calculated as $E_{nx}=U_x-B_x$. In this way we obtained the $\nu_x(E_{nx})$ functions for xth chance fission.

To calculate $\nu(E_n)$ at incident neutron energies $E_n\gtrsim E_{nnf}$ we used relevant low-energy data for the nuclei involved in the multiple-chance fission reactions. The systematic approach of Ref. [44] was employed to estimate the energy dependence of the number of prompt fission neutrons $\nu_x(E_n)$ for $^{238}\mathrm{U}(n,f)$, $^{237}\mathrm{U}(n,f)$, $^{236}\mathrm{U}(n,f)$, and $^{235}\mathrm{U}(n,f)$ reactions up to the relevant emissive fission thresholds. Calculated neutron multiplicity is compatible with the measured data on $\nu(E_n)$ by Frehaut [45] in the energy range $E_n\sim 8-20$ MeV. It is compared with the measured data [45–50] in Fig. 9. Small discrepancies of calculated and measured data are noticed at low energies, since adopted approximation ignores changes of the slope of $\nu(E_n)$ in the first plateau region (see Fig. 9), and above $E_n\sim 16$ MeV, but they are well within the data scatter. Figure 9 shows also partial contributions of the emissive fission reactions $^{238}\mathrm{U}(n,xnf)$ to the prompt fission neutron number of $^{238}\mathrm{U}(n,F)$ reaction.

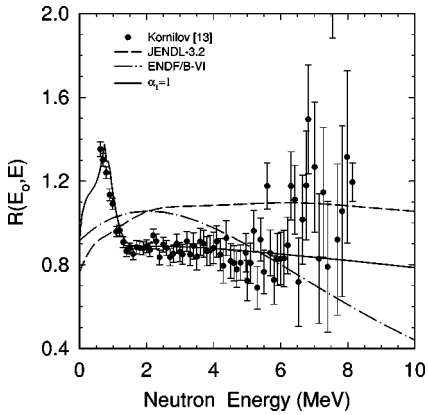

FIG. 12. Measured and calculated $^{238}\mathrm{U}(n,F)$ reaction PFNS at $E_n=7$ MeV relative to Maxwell PFNS with the average energy $\langle E\rangle=2.0242$ MeV.

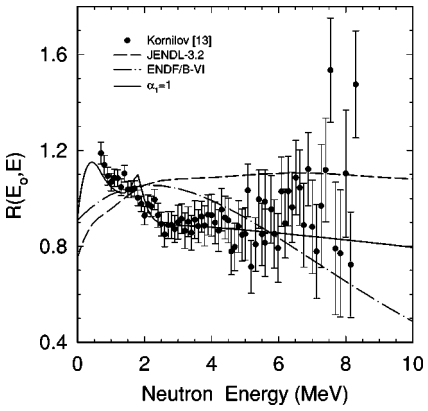

FIG. 13. Measured and calculated ^{238}U(n,F) reaction PFNS at E_n=8 MeV relative to Maxwell PFNS with the average energy $\langle E\rangle$=2.0461 MeV.

To calculate the $\nu(E_n)$ for the ^{232}Th(n,F) reaction up to $E_n \sim 20$ MeV we should know $\nu_x(E_n)$ for ^{231}Th(n,f), ^{230}Th(n,f), and ^{229}Th(n,f) reactions, which contribute to the observed $\nu(E_n)$ via emissive ^{232}Th(n,xnf) fission reactions. We described the energy dependence of $\nu_1(E_n)$ for the first-chance fission of ^{232}Th(n,f) reaction [51–65] using two energy intervals — from the thermal energy point up to E_n =3.8 MeV and from E_n=3.8 up to E_n=6 MeV. The slope of linear fit in the first energy interval was chosen to describe the experimental data in MeV-energy region together with the thermal point ν value (2.175) for ^{232}Th(n,f). Then we fixed ν value (2.327) at 3.8 MeV and defined the slope for the second energy interval (E_n=3.8–6 MeV). This calculation is shown as a solid line in Fig. 10. We applied the same approach in case of ^{229,230,231}Th isotopes also, but the energy dependencies were shifted according to the thermal values of prompt fission neutron number ν_{th}. Thermal point values of ν_x were taken from the systematics by Malinovskij [44]. Figure 10 shows also partial contributions to the observed prompt fission number up to E_n=20 MeV. Bump in $\nu(E_n)$ around (n,nf) reaction threshold is due to the prefission neutrons emitted in ^{232}Th(n,nf) reaction, in case of ^{238}U(n,nf) reaction it is almost unpronounced.

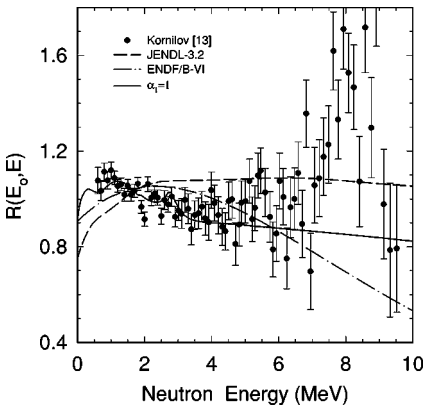

FIG. 14. Measured and calculated ^{238}U(n,F) reaction PFNS at E_n=9 MeV relative to Maxwell PFNS with the average energy $\langle E\rangle$=2.0757 MeV.

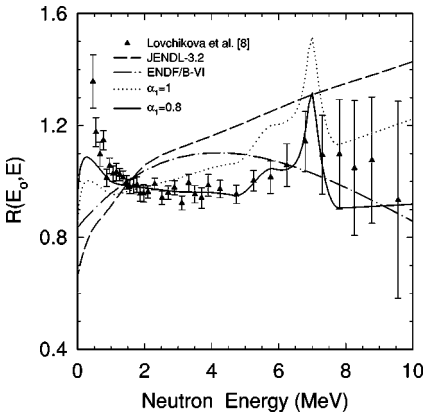

FIG. 15. Measured and calculated ^{238}U(n,F) reaction PFNS at E_n=13.2 MeV relative to Maxwell PFNS with the average energy $\langle E\rangle$=2.0415 MeV. Solid line corresponds to α_1=0.8, resembling c.m.s. energy reduction; dashed line corresponds to α_1=1.

IV. MEASURED PFNS DATA ANALYSIS

Figures 11–20 show PFNS measured data for ^{238}U(n,f) and ^{232}Th(n,f) reactions at $E_n \sim 6-17.7$ MeV and calculated PFNS. Data points as well as the calculated curves are shown relative to the Maxwell distributions with various average energies, indicated in figure captions, PFNS of evaluated data files of ENDF/B-VI [66] and JENDL-3.2 [67] data libraries are also shown. For ^{238}U(n,f) reaction Figs. 11–14 show the variation of the $(n,nf)^1$ neutron contribution to the observed PFNS with the increase of $E_{th} \sim E_n - B_f$ energy. It looks like a wave, moving from the left to the right side of the plots. With further increase of E_n (see Figs. 15–18, actually above $(n,2nf)$ emissive fission threshold, calculated curves resemble the $(n,nf)^1$ spectra contributions to the PFNS, but generally, calculated PFNS seem to be systematically higher than PFNS data for $\varepsilon \gtrsim 2$ MeV and lower for $\varepsilon \lesssim 2$ MeV (see dotted curves in Figs. 15–18, labeled "α_1 =1").

We would try to reconcile measured and calculated prompt fission neutron spectra above $(n,2nf)$ emissive fis-

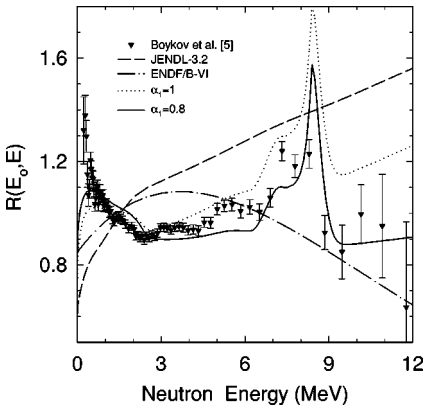

FIG. 16. Measured and calculated ^{238}U(n,F) reaction PFNS at E_n=14.7 MeV relative to Maxwell PFNS with the average energy $\langle E\rangle$=2.0456 MeV. Solid line corresponds to α_1=0.8, resembling c.m.s. energy reduction; dashed line corresponds to α_1=1.

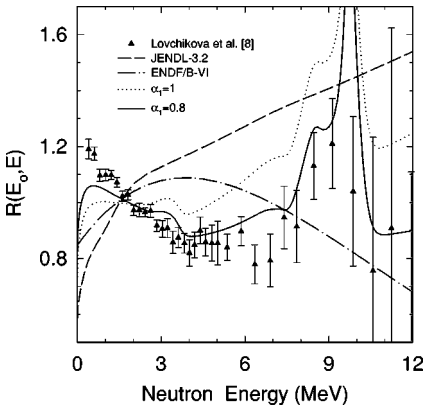

FIG. 17. Measured and calculated ^{238}U(n,F) reaction PFNS at E_n=16 MeV relative to Maxwell PFNS with the average energy $\langle E\rangle$=2.0584 MeV. Solid line corresponds to α_1=0.8, resembling c.m.s. energy reduction; dashed line corresponds to α_1=1.

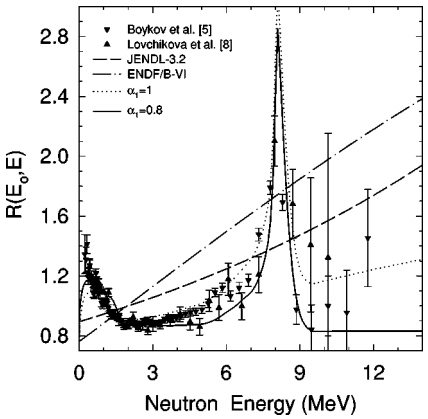

FIG. 19. Measured and calculated ^{232}Th(n,F) reaction PFNS at E_n=14.7 MeV relative to Maxwell PFNS with the average energy $\langle E\rangle$=1.9456 MeV. Solid line corresponds to α_1=0.8, resembling c.m.s. energy reduction; dashed line corresponds to α_1=1.

sion threshold using the following arguments. It was shown by Eismont [68] that at incident neutron energy $E_n \sim 14$ MeV total excitation energy of separated fission fragments might be rather high. Consequently, neutron emission time might be comparable to the fragment acceleration time $\sim 10^{-20}$ s. That means some neutrons could be emitted during fragment acceleration. Consequently, the c.m.s. energy and average neutron energy in the LS system [69,70] would be further reduced. For preacceleration neutron emission one could assume the dependence of the TKE on the emission time [69,70]. Let us introduce the ratio of the total kinetic energies at time t and at infinity, $\alpha(t)=\mathrm{TKE}(t)/TKE_\infty$. One may assume that neutron emission from an excited fragment is described by the exponential law with life-time τ. The average value $\langle\alpha(\tau)\rangle$ [70] may be estimated as

$$\langle\alpha(\tau)\rangle = \frac{1}{\tau}\int \alpha(t)\exp(-t/\tau)dt. \tag{25}$$

After emission of the first neutron, the fragment excitation energy is reduced and the emission time increases, i.e., for all neutrons emitted after the first one, we assume $\alpha \sim 1$. Thus, we could estimate "observed" α value as

$$\alpha_{obs} = \nu^{-1}[\langle\alpha(\tau)\rangle + (\nu-1)], \tag{26}$$

where $\nu \sim 2$ is the total number of neutrons emitted from the fragment. It was shown in Ref. [70] that if emission time equals $\tau \sim (1-2)\times 10^{-20}$ s, then $\alpha_{obs} \sim 0.9$. It is rather difficult to estimate the neutron lifetime reliably, it depends on the model assumptions (level density parameters, excitation energy, etc.). For the Mo-Ba and Tc-Cs fission fragments in spontaneous fission of ^{252}Cf (total excitation energy $E_x^* \sim 33$ MeV), ~60% of these fragments may be attributed $\tau \sim 2\times 10^{-20}$ s and ~40% of fission fragments may be attributed $\tau \sim 1\times 10^{-19}$ s. Hence, one may expect that the actual correction due to the preacceleration emission will be $\alpha_{obs} \lesssim 0.9$, if $E_x^* \gtrsim 35$ MeV. For ^{238}U(n,F) fission reaction at $E_n \sim 14$ MeV excitation energies are E_x^* =35.1, 27.8, 21.8, and 16.6 MeV for ^{238}U(n,f), ^{238}U(n,nf), ^{238}U$(n,2nf)$, and ^{238}U$(n,3nf)$ fission reactions, respectively. Considering only the influence of excitation ener-

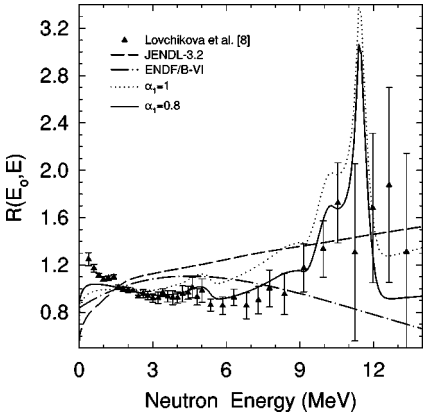

FIG. 18. Measured and calculated ^{238}U(n,F) reaction PFNS at E_n=17.7 MeV relative to Maxwell PFNS with the average energy $\langle E\rangle$=2.0878 MeV. Solid line corresponds to α_1=0.8, resembling c.m.s. energy reduction; dashed line corresponds to α_1=1.

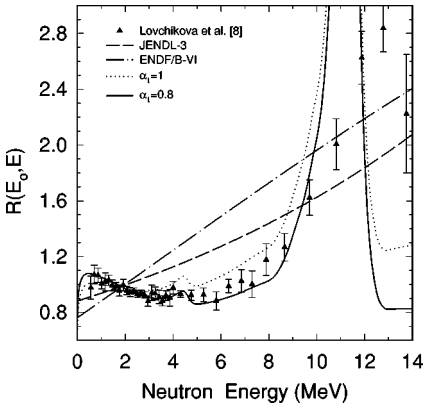

FIG. 20. Measured and calculated ^{232}Th(n,F) reaction PFNS at E_n=17.7 MeV relative to Maxwell PFNS with the average energy $\langle E\rangle$=1.9749 MeV. Solid line corresponds to α_1=0.8, resembling c.m.s. energy reduction; dashed line corresponds to α_1=1.

gies on the emission process, $\alpha_{obs} \sim 0.9$ could be estimated due to the preacceleration emission. We employ the present approach, having in mind that it is at least a semi-empirical parametrization of measured PFNS data. We could reproduce measured PFNS data assuming that c.m.s. energy per nucleon, E_{vo}, is further reduced as

$$\overline{E}_{\nu ij} = \alpha_1 \widetilde{E}_{\nu ij}. \tag{27}$$

We suppose that $\alpha_1 = 1$ for $E_n < 10$ MeV and $\alpha_1 = 0.8$ for $E_n > 12$ MeV and is linearly interpolated in between. This additional correction of the average energy of postfission neutrons removes much of the discrepancies of calculated spectra with measured PFNS data at $E_n = 13.2$, 14.7, 16, and 17.7 MeV (see solid lines in Figs. 15–18). PFNS data for the ^{238}U(n,f) reaction at $E_n = 13.2$ MeV (Fig. 15) are nicely reproduced. For $E_n = 14.7$ MeV (see Fig. 16) increase of E_{th} for $(n,nf)^1$ reaction spectra is reproduced, we might assume that change of the data shape around $\varepsilon \sim 2$ MeV is due to the sharp decrease of the first neutron spectrum contribution of $(n,2nf)^1$ reaction to the observed PFNS. For still higher incident neutron energies $E_n = 16$ MeV (Fig. 17) and $E_n = 17.7$ MeV (Fig. 18) irregularities in measured PFNS data around $\varepsilon \sim 3$ MeV and $\varepsilon \sim 5$ MeV, respectively, also might be attributed to the $(n,2nf)^1$ spectrum contribution. Irregularities due to the $(n,nf)^1$ neutron contributions around $\varepsilon \sim E_{th} = E_n - B_f$ also are well reproduced. However, some excess of the soft neutrons with $\varepsilon \lesssim 0.5$ MeV is still observed, but it is much lower than in previous evaluations of ENDF/B-VI [66] and JENDL-3.2 [67].

The peculiarities of the same nature are evidenced in case of ^{232}Th(n,f) PFNS data analysis. For the incident neutron energy $E_n = 14.7$ MeV (see Fig. 19) peak in PFNS at $\varepsilon \sim E_{th} \sim 8$ MeV is well reproduced. Slight excess of the soft neutrons is still observed only for $\varepsilon \lesssim 0.5$ MeV. For $E_n = 17.7$ MeV there are no data points below $\varepsilon \sim 0.5$ MeV to notify excess of soft neutrons, unlike ^{238}U(n,f) reaction. Irregularity around $\varepsilon \sim 5$ MeV, which could be attributed to the $(n,2nf)^1$ neutrons, i.e., first neutrons of $(n,2nf)$ reaction, is also reproduced quite well. As regards a peak in PFNS due to the $(n,nf)^1$ neutrons, we argue that it should be at lower energy $\varepsilon \sim E_{th} \sim 11$ MeV, instead of $\varepsilon \sim 12.5$ MeV. Moreover, the peak should be higher than that observed in measured PFNS data. We argue that for the observed PFNS of ^{232}Th(n,f) at $E_n \sim 17.7$ and $E_n \sim 14.7$ MeV the contribution of $(n,nf)^1$ spectra should produce much stronger peaks around $\varepsilon \sim E_n - B_f$ energy than in case of ^{238}U(n,f) reaction. This is explained by the fact that peak in the shape of the fission probability of ^{232}Th nuclide is stronger than that of ^{238}U. This conclusion is supported by good fits of PFNS data at $E_n \sim 14.7$ MeV, both for ^{232}Th(n,f) (see Fig. 19) and ^{238}U(n,f) (see Fig. 16) reactions.

Decomposition of the observed prompt fission neutron spectra into contributions from multiple-chance fission [see Eq. (19)] allows to deconvolute the observed prompt fission neutron spectrum into contributions coming from nonemissive fission of $A+1$ nucleus $\widetilde{S}_{A+1}(E_n,\varepsilon)$, second-chance fission—$(n,nf)$-reaction neutrons and neutrons, evaporated from the fission fragments of A nucleus $\widetilde{S}_A(E_n,\varepsilon)$, third-chance fission—$(n,2nf)$-reaction neutrons and neutrons, evaporated from the fission fragments of $A-1$ nucleus $\widetilde{S}_{A-1}(E_n,\varepsilon)$, and fourth-chance fission—$(n,3nf)$-reaction neutrons and neutrons, evaporated from the fission fragments of $A-2$ nucleus $\widetilde{S}_{A-2}(E_n,\varepsilon)$. Figures 21 and 22 show contributions from the multiple-chance fission at $E_n = 20$ MeV for ^{238}U(n,f) and ^{232}Th(n,f) reactions, respectively.

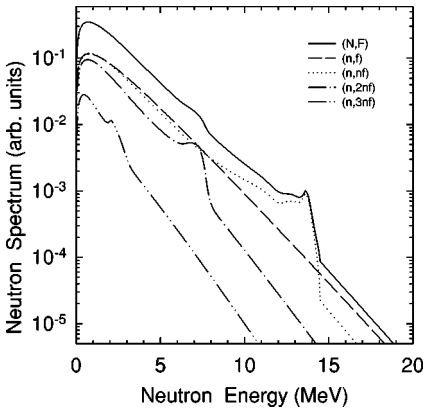

FIG. 21. Multiple-chance fission contributions to the prompt fission neutron spectrum for ^{238}U(n,F) reaction.

In case of ^{238}U(n,f) reaction contributions from the first- and second-chance fission reactions are comparable for prompt fission neutron energies $\varepsilon \lesssim 8$ MeV. For higher emitted neutron energies, contribution of (n,nf)-reaction neutrons produces a plateau and a peak in observed PFNS (see Fig. 21). This contribution fades at $\varepsilon \gtrsim 14.5$ MeV, at higher ε values only neutrons from fission fragments of fission of ^{238}U nuclide contribute to $\widetilde{S}_A(E_n,\varepsilon)$. Contribution coming from ^{238}U$(n,2nf)$ fission reaction $\widetilde{S}_{A-1}(E_n,\varepsilon)$ is lower than those of ^{238}U(n,f) and ^{238}U(n,nf) reactions, i.e., $\widetilde{S}_{A+1}(E_n,\varepsilon)$ and $\widetilde{S}_A(E_n,\varepsilon)$, respectively. A broad step around $\varepsilon \sim 7$ MeV is due to the contribution of the first neutron of $(n,2nf)$ reaction, it fades out at higher ε values. The same peculiarity in $\widetilde{S}_{A-2}(E_n,\varepsilon)$, which is less pronounced, is due to the con-

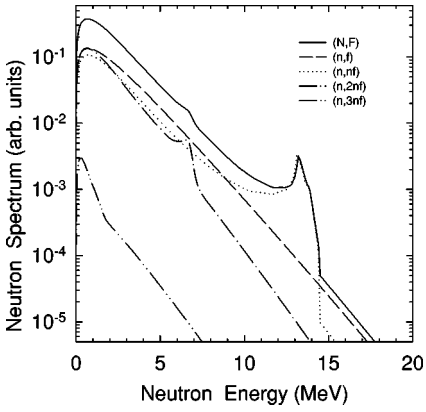

FIG. 22. Multiple-chance fission contributions to the prompt fission neutron spectrum for ^{232}Th(n,F) reaction.

tribution of the first neutron of $(n,3nf)$ reaction.

In case of ^{232}Th(n,f) reaction $\widetilde{S}_{A+1}(E_n,\varepsilon)$, the contribution from first-chance fission is generally higher than that of second-chance fission reaction $\widetilde{S}_A(E_n,\varepsilon)$, except the prompt fission neutron energy range of $\varepsilon\sim 9-14.5$ MeV (see Fig. 22). In this energy range a large contribution to the observed PFNS comes from the prefission (n,nf) reaction neutrons. Below $\varepsilon\sim 2$ MeV, contribution of the third-chance fission $\widetilde{S}_{A-2}(E_n,\varepsilon)$ is even higher than that of the second-chance fission $\widetilde{S}_{A-1}(E_n,\varepsilon)$, for higher energies of prompt fission neutrons, i.e., $\varepsilon\gtrsim 6$ MeV, it is much lower. Contribution of the fourth-chance fission $\widetilde{S}_{A-2}(E_n,\varepsilon)$ is rather low, it is much lower than in case of ^{238}U(n,f) reaction. For emitted neutron energies higher than $\varepsilon\sim 10$ MeV, contribution of the (n,nf)-reaction neutrons produces a plateau and a peak in observed PFNS, which is larger than in case of ^{238}U(n,f) reaction. Structure in prompt fission neutron spectrum, coming from the third-chance fission, i.e., first neutron of $(n,2nf)$ reaction, is less pronounced than in case of ^{238}U(n,f) reaction. For incident neutron energies $E_n\gtrsim E_{n2nf}$ one faces some excess of the soft neutrons in PFNS data for ^{238}U(n,f) reaction, as compared with the model calculations. In case of lower fissility target nuclide ^{232}Th there is no soft neutron excess at $E_n\sim 17.7$ MeV, at $E_n\sim 14.7$ MeV the excess is somewhat lower than in case of ^{238}U target nuclide.

V. CONCLUSION

Analysis of measured ^{238}U(n,f) and ^{232}Th(n,f) PFNS data showed that a number of data peculiarities could be correlated with the influence of (n,xnf) prefission neutron spectra on the observed prompt fission neutron spectra, neutron spectra from the fission fragments being described with Watt distributions. To describe PFNS data shapes for incident neutron energies higher than $(n,2nf)$ emissive fission threshold, the reduction of the c.m.s. velocity due to the neutron emission during fragment acceleration was assumed. The lowering of the Watt distribution energy parameter, c.m.s. energy per nucleon, allowed to describe PFNS data shapes for prompt fission neutron energies $\varepsilon\gtrsim 0.5$ MeV. For ^{238}U(n,f) reaction the excess of soft neutrons at $E_n=14.7$ MeV is lower than in case of ^{238}U(n,f) reaction, at $E_n=17.7$ MeV it almost disappears.

The increase of the cutoff energy $E_{th}\sim E_n-B_f$ of the (n,nf) reaction neutron spectra with excitation energy of fissioning nucleus is reproduced for $E_n\sim 6-18$ MeV. A steplike irregularity around emitted neutron energy $\varepsilon\sim 3-5$ MeV for E_n above $(n,2nf)$ reaction threshold could be correlated with the first neutron spectrum of ^{238}U$(n,2nf)$ reaction and ^{232}Th$(n,2nf)$. Multiple-chance fission structure was obtained by the self-consistent description of ^{238}U(n,f), ^{238}U$(n,2n)$, ^{238}U$(n,3n)$ and ^{232}Th(n,f), ^{232}Th$(n,2n)$ reaction cross sections.

Summarizing, we argue that correct estimates of the prefission (n,xnf) reaction spectra, alongside simple modeling of spectra of neutrons emitted from the fission fragments, allow to reproduce a number of peculiarities in measured prompt fission neutron spectra. Though the absolute value of the correction of the total kinetic energy at the moment of neutron emission is somewhat larger than the values that could be estimated using the excitation energy and acceleration time of the fission fragments, the present approach provides a versatile theoretical tool for the measured PFNS data analysis and PFNS prediction for the target nuclides with various fissilities.

ACKNOWLEDGMENTS

The Research was supported by the International Science and Technology Center under the Project Agreement B-404 (the Funding Party for the Project is Japan) and International Atomic Energy Agency (Vienna, Austria) under Research Contract No. 12353.

[1] J. W. Negele, S. E. Koonin, P. Moller, J. R. Nix, and A. J. Sierk, Phys. Rev. C **17**, 1098 (1978).
[2] Y. Boneh and Z. Fraenkel, Phys. Rev. C **10**, 893 (1974).
[3] C. Budtz-Jorgensen and H.-H. Knitter, Nucl. Phys. **A490**, 307 (1988).
[4] D. Hilscher and H. Rossner, Ann. Phys. (Paris) **17**, 471 (1992).
[5] G. S. Boykov, V. D. Dmitriev, G. A. Kudyaev, Yu. B. Ostapenko, M. I. Svirin, and G. N. Smirenkin, Yad. Fiz. **53**, 628 (1991).
[6] G. S. Boykov, V. D. Dmitriev, G. A. Kudyaev, Yu. B. Ostapenko, M. I. Svirin, and G. N. Smirenkin, Phys. At. Nucl. **57**, 2047 (1994).
[7] G. N. Smirenkin, G. N. Lovchikova, A. M. Trufanov, M. I. Svirin, A. V. Polyakov, V. A. Vinogradov, V. D. Dmitriev, and G. S. Boykov, Yad. Fiz. **59**, 1934 (1996).
[8] G. N. Lovchikova, A. M. Trufanov, M. I. Svirin, A. V. Polyakov, V. A. Vinogradov, V. D. Dmitriev, and G. S. Boykov, in *Proceedings of the XIV International Workshop on Nuclear Fission Physics, Obninsk, 2000*, edited by B. I. Fursov, A. A. Goverdovski, and V. V. Ketlerov (State Scientific Center of Russian Federation-Institute for Physics & Power Engineering (SSC RFIPPE), Obninsk, pp. 72–82.
[9] V. M. Maslov, Yu. V. Porodzinskij, M. Baba, A. Hasegava, N. V. Kornilov, A. B. Kagalenko, and N. A. Tetereva, Eur. Phys. J. A **18**, 93 (2003).
[10] Yu. S. Zamiatnin, I. N. Safina, E. K. Tutnikova, and N. I. Ivanova, At. Energ. **4**, 337 (1958).
[11] V. Ya. Baryba, N. V. Kornilov, and O. A. Sal'nikov, Preprint FEI-947, 1979.
[12] N. V. Kornilov, B. V. Zhuravlev, O. A. Salnikov, and V. I. Trykova, in *Proceedings of the 5th Conference on Neutron Physics, Kiev, 1980*, edited by L. N. Usachev (Tsniiatominform, Moscow, USSR, 1980), Vol. 2, p. 44.
[13] N. V. Kornilov, Vopr. At. Nauki Tekh., Ser.: Yad. Konstanty **4**, 46 (1985).

[14] M. I. Svirin, G. N. Lovchikova, and A. M. Trufanov, Yad. Fiz. **60**, 818 (1997).
[15] T. Kawano, T. Ohsawa, M. Baba, and T. Nakagawa, Phys. Rev. C **63**, 034601 (2001).
[16] D. C. Madland and J. R. Nix, Nucl. Sci. Eng. **81**, 213 (1982).
[17] V. M. Maslov, Yu. V. Porodzinskij, A. Hasegawa, M. Baba, N. V. Kornilov, and A. B. Kagalenko, in *Proceedings 10th International Seminar on Interaction of Neutrons with Nuclei, Dubna 2002*, edited by A. M.Sukhovoj (JINR, Russia, 2003).
[18] V. M. Maslov, in *Nuclear Reaction Data and Nuclear Reactors* (ICTP, 2001), p. 231.
[19] M. Uhl and B. Strohmaier, IRK-76/01, 1976.
[20] V. M. Strutinsky, Nucl. Phys. **A95**, 420 (1967).
[21] S. Bjørnholm and J. E. Lynn, Rev. Mod. Phys. **52**, 725 (1980).
[22] H. Weigmann, in *The Fission Process*, edited by C. Wagemans (CRC, Boca Raton, 1991).
[23] J. W. Behrens and G. W. Carlson, Nucl. Sci. Eng. **63**, 250 (1977).
[24] B. I. Fursov, V. H. Kupriyanov, B. K. Maslennikov, and G. N. Smirenkin, Sov. At. Energy **43**, 808 (1978).
[25] J. W. Meadows, Nucl. Sci. Eng. **58**, 255 (1975).
[26] P. E. Vorotnikov, S. M. Dubrovina, G. A. Otroshchenko, and V. A. Shigin, Yaderno-Physycheskie Issledovaniya **12**, 22 (1971).
[27] I. D. Alkhazov, V. P. Kasatkin, O. I. Kostochkin, L. S. Malkin, A. V. Sorokina, K. A. Petrzhak, A. V. Fomichev, V. I. Shpakov, B. V. Rumjantsev, and A. M. Sokolov, in *Neutron Physics, Proceeding of All-Union Conference*, edited by L. N. Usachev (Tsniiatominform, Moscow, 1973), Vol. 4, p. 13.
[28] P. W. Lisowski, A. Gavron, W. E. Parker, J. L. Ullmann, S. J. Balestrini, A. D. Carlson, O. A. Wasson, and N. W. Hill, in *Proceeding of Specialists' Meeting on Neutron Cross Section Standards for the Energy Region above 20 MeV, Uppsala, Sweden, 1991* (Nuclear Energy Agency (NEA) OECD, Paris, 1991), p. 177.
[29] V. M. Maslov, Yu. V. Porodzinskij, M. Baba, A. Hasegava, N. V. Kornilov, A. B. Kagalenko, and N. A. Tetereva, INDC(BLR)-14, 2003.
[30] B. I. Fursov, E. Yu. Baranov, M. P. Klemyshev, B. F. Samylin, G. N. Smirenkin, and Yu. M. Turchin, At. Energ. **71**, 320 (1991).
[31] J. W. Meadows, in *International Conference on Nuclear Cross Sections for Technology, Knoxville, Tennessee, 1979*, edited by J. W. Fowler, G. H. Johnson, and C. D. Bowman, National Bureau of Standards Special Publication NBS SP-594 (U.S. Government Pringing Office, Washington, DC , 1980), p. 479.
[32] K. Kanda, H. Imaruoka, K. Yoshida, O. Sato, and N. Hirakawa, Radiat. Eff. **93**, 233 (1986).
[33] J. W. Behrens, J. C. Browne, and E. Ables, Nucl. Sci. Eng. **81**, 512 (1982).
[34] A. A. Goverdovskij, A. K. Gordjushin, B. D. Kuz'minov, V. F. Mitrofanov, and A. I. Sergachev, At. Energ. **60**, 416 (1986).
[35] A. A. Goverdovskij, A. K. Gordjushin, B. D. Kuz'minov, V. F. Mitrofanov, A. I. Sergachev, S. M. Solov'ev, and T. E. Kuz'mina, At. Energ. **61**, 380 (1986).
[36] J. W. Meadows, Ann. Nucl. Energy **15**, 421 (1988).
[37] O. A. Shcherbakov, A. Donets, A. Evdokimov, A. Fomichev, T. Fukahori, A. Hasegava, A. Laptev, V. Maslov, G. Petrov, S. Soloviev, Yu. Tuboltsev, and A. Vorobyev, in *Proceedings of the International Conference on Nuclear Data for Science and Technology, Tsukuba, Japan, 2001*, edited by K. Shibata (Atomic Energy Society, Japan, 2001), p. 230.
[38] V. M. Maslov, Yu. V. Porodzinskij, M. Baba, A. Hasegava, N. V. Kornilov, A. B. Kagalenko, and N. A. Tetereva, INDC(BLR)-16, 2003.
[39] V. M. Maslov, Ann. Nucl. Energy **19**, 181 (1992).
[40] C. K. Cline, Nucl. Phys. **A195**, 353 (1972).
[41] E. Gadioli, E. Gadioli Erba, and P. G. Sona, Nucl. Phys. **A217**, 589 (1973).
[42] N. V. Kornilov, A. B. Kagalenko, V. M. Maslov, and Yu. V. Porodzinskij, *Nuclear Data for Science and Technology*, edited by J. Reffo, A. Ventura, and G. Grandi (Italian Physical Society, Bologna, 1997), Vol. 1, p. 940.
[43] N. V. Kornilov, A. B. Kagalenko, and F.-J. Hambsch, Phys. At. Nucl. **62**, 173 (1999).
[44] V. V. Malinovskij, Vopr. At. Nauki Tekh., Ser.: Yad. Konstanty **2**, 25 (1987).
[45] J. Frehaut, NEANDC(E) 238/L, 1986.
[46] B. Nurpeisov, K. E. Volodin, V. G. Nesterov, L. I. Prokhorova, G. N. Smirenkin, and Yu. M. Turchin, At. Energ. **39**, 199 (1975).
[47] V. V. Malinovskij, B. D. Kuz'minov, and V. G. Vorob'jova, Vopr. At. Nauki Tekh., Ser.: Yad. Konstanty **50**, 4 (1983).
[48] V. G. Vorob'jova, N. P. D'jachenko, B. D. Kuz'minov, and A. I. Sergachjov, Vopr. At. Nauki Tekh., Ser.: Yad. Konstanty **15**, 3 (1974).
[49] M. U. Savin, Yu. Khokhlov, I. N. Paramonova, and V. A. Chirkin, At. Energ. **32**, 408 (1972).
[50] Bao Zongyu, Atomic Energy Science and Technology **9**, 362 (1975).
[51] L. E. Glendenin, J. E. Gindler, I. Ahmad, D. J. Henderson, and J. W. Meadows, Phys. Rev. C **22**, 152 (1980).
[52] R. E. Howe, Nucl. Sci. Eng. **86**, 157 (1984).
[53] H. Conde and M. Holmberg, Ark. Fys. **29**, 33 (1965).
[54] R. Batchelor, W. B. Gilboy, and J. H. Towle, Nucl. Phys. **65**, 236 (1965).
[55] D. S. Mather, P. Fieldhouse, and A. Moat, Nucl. Phys. **66**, 149 (1965).
[56] J. Frehaut, R. Bois, and A. Bertin, Report of CEA-N-2196 1981.
[57] J. Caruana, J. W. Boldeman, and R. L. Walsh, Nucl. Phys. **A285**, 217 (1977).
[58] L. I. Prokhorova and G. N. Smirenkin, Sov. J. Nucl. Phys. **7**, 579 (1968).
[59] V. V. Malinovskyj, V. G. Vorobjova, B. D. Kuzminov, V. M. Piksajkin, N. N. Semjonova, V. S. Valjavkin, and S. M. Solovjov, At. Energ. **54**, 209 (1983).
[60] B. D. Kuzminov, Sov. J. Nucl. Phys. **4**, 241 (1961).
[61] A. B. Smith, R. G. Nobles, and S. A. Cox, Phys. Rev. **115**, 1242 (1959).
[62] I. I. Bondarenko, B. D. Kuzminov, L. S. Kutsayeva, L. I. Prokhorova, and G. N. Smirenkin (unpublished).
[63] J. Leroy, J. Phys. Radium **21**, 617 (1960).
[64] C. Feu, Journ. de Physique **38**, 273 (1977).
[65] I. Johnstone, Report No. AERE-NP/R-1912, 1956.
[66] R. W. Roussin, P. G. Young, and R. McKnight, in *Proceedings of the International Conference on Nuclear Data for Science and Technology, Gatlinburg, USA, 1994*, edited by J. K. Dickens (ANS, La Grange Park, 1994), p. 692.
[67] JAERI-Data/Code, 98-006 (Part II), 1998.

[68] V. P. Eismont, At. Energ. **9**, 113 (1965).
[69] N. V. Kornilov and A. B. Kagalenko, in *Proceedings of the II International Seminar on Interaction of Neutrons with Nuclei, Dubna, 1994*, edited by A. M. Sukhovoj (JINR, Russia), p. 116.
[70] H.-H. Knitter, U. Brosa, and C. Budtz-Jorgensen, in *Neutron and Gamma Emission in Fission*, edited by C. Wagemans (CRC, Boca Raton, 1991).